Density Profiles in Thin PMMA Supported Films Investigated by X-ray Reflectometry

ARTICLE *in* LANGMUIR · NOVEMBER 2001

Impact Factor: 4.46 · DOI: 10.1021/la010811w

Density Profiles in Thin PMMA Supported Films Investigated by X-ray Reflectometry

A. van der Lee,[†] L. Hamon,[‡] Y. Holl,[‡] and Y. Grohens*,[§]

Institut Européen des Membranes, Université de Montpellier II - cc 047, 2 place E. Bataillon, 34095 Montpellier Cedex 5, France, Institut de Chimie des Surfaces et Interfaces-CNRS, 15, rue J.Starcky, BP 2488, 68057 Mulhouse Cedex, France, and Laboratoire Polymères et Procédés, Université de Bretagne-Sud, Centre de Recherche, rue Saint-Maudé, 56325 Lorient, France

Received June 4, 2001. In Final Form: September 3, 2001

We have investigated the electron density profiles normal to the substrate of 20−80 nm thick films of stereoregular poly(methyl methacrylate) (PMMA) spin-cast on silicon wafers by X-ray reflectometry. The reflectivity curves were analyzed using a least-squares procedure based on the distorted-wave Born approximation that is capable of modeling slight density fluctuations. From the calculated electronic density profiles, an increase in the density in the vicinity of the solid SiO_x surface can be observed regardless of PMMA film thickness and tacticity. This result is discussed in terms of local molecular packing near surfaces. Moreover, small periodic density fluctuations appeared for film thicknesses above 30 nm. These are tentatively attributed to a layering formation due to both fast solvent evaporation and polymer autophobicity during the spin-coating process. This layering effect is compared to that observed after freeze-drying of a semidilute solution where fast evaporation limits the interpenetration of polymer coils in the thin film.

Introduction

In recent years, there has been much interest in the peculiar properties of thin polymer films.[1−10] These thin films are of growing interest in industrial applications such as electronic packaging, protective coating, and biocompatible surfaces. The constraints generated by the presence of two interfaces have been shown to modify profoundly the conformation,[1] the dynamics,[2] or the dewetting behavior[3] of the polymer chains.

The glass transition temperature of thin layers, Tg(h), of polymers has been investigated by many groups in the past few years.[4−10] One of the main conclusions drawn from these works is that the Tg(h) of thin films decreases for weakly interacting systems[4,5,7] and increases on strongly attractive surfaces.[5−8] In the case of freely standing PS films, Tg(h) decreases much more rapidly with decreasing film thickness than for supported films.[4] Polymers at free surfaces or in contact with repulsive surfaces are claimed to be dominated by entropic effects such as disentanglements, confinement effects, chain-end segregation, or specific motion such as sliding motion[9] which leads to a Tg(h) depression.[10] In contrast, the increase of Tg for poly(methyl methacrylate) (PMMA) or poly-2-vinylpyridine (P2VP) thin layers, as occurs on strongly attractive substrates, is often ascribed to specific chain organization (interactions, conformation, orientation).[11] Changing the PMMA tacticity has been demonstrated to increase the Tg(h) for isotactic PMMA while depressing it for the syndiotactic isomer when decreasing the film thickness below 50 nm. This behavior, specifically dependent on the PMMA microstructure, was assumed to be influenced by the density of specific interactions of stereoregular chains with the aluminum surface which influences the local molecular packing at interfaces.[12]

X-ray and neutron reflectivity studies on thin polymer layers have been performed before. Most studies have concentrated either on the width of the interface between substrate and film[13−16] or on the film thickness dependent thermal properties of different polymers.[17−20] Normally, it is assumed that the electronic or mass density remains essentially constant normal to the surface; it was explicitly

* To whom correspondence should be addressed: E-mail: yves.grohens@univ-ubs.fr.

[†] Institut Européen des Membranes, Université de Montpellier II.

[‡] Institut de Chimie des Surfaces et Interfaces-CNRS.

[§] Laboratoire Polymères et Procédés, Université de Bretagne-Sud.

(1) Konstadinis, K.; Thakkar, B.; Chakraborty, A.; Potts, L. W.; Tannenbaum, R.; Tirrell, M.; Evans, J. F. *Langmuir* **1992**, *8*, 1307.

(2) Israelachvili, J.; McGuiggan, P.; Gee, M.; Homola, A.; Robbins, M.; Thompson, P. *J. Phys.: Condens. Matter* **1990**, *2*, 89.

(3) Reiter, G. *Macromolecules* **1994**, *27*, 3046.

(4) Keddie, J. L.; Jones, R. A. L.; Cory, R. A. *Europhys. Lett.* **1994**, *27*, 59.

(5) Keddie, J. L.; Jones, R. A. L.; Cory, R. A. *Faraday Discuss.* **1994**, *98*, 219.

(6) Forrest, J. A.; Dalnoki-Veress, K.; Stevens, J. R.; Dutcher, J. R. *Phys. Rev. Lett.* **1996**, *77*, 2002.

(7) van Zanten, J. H.; Wallace, W. E.; Wu, W. L. *Phys. Rev. E* **1996**, *53* (3), R2053.

(8) Brown, H. R.; Russel, T. P. *Macromolecules* **1996**, *29*, 798.

(9) De Gennes, P. G. *Eur. Phys. J. E* **2000**, *2*, 201.

(10) Kajiyama, T.; Tanaka, K.; Takahara, A. *Macromolecules* **1997**, *30*, 280.

(11) Wu, W.-L.; Majkrazak, C. F.; Satija, S. K.; Ankner, J. F.; Orts, W. J.; Satkowski, M.; Smith, S. D. *Polymer* **1992**, *33*, 5081.

(12) Grohens, Y.; Brogly, M.; Labbe, C.; David, M.O.; Schultz, J. *Langmuir* **1998**, *14*, 2929.

(13) Lin, E. K.; Wu, W.-L.; Satija, S. K. *Macromolecules* **1999**, *30*, 77224.

(14) Lin, E. K.; Kolb, R.; Satija, S. K.; Wu, W.-L. *Macromolecules* **1999**, *32*, 3753.

(15) Bollinne, C.; Stone, V. W.; Carlier, V.; Jonas, A. M. *Macromolecules* **1999**, *32*, 4719.

(16) Sferrazza, M.; Jones, R. A. L.; Penfold, J.; Bucknall, D. B.; Webster, J. R. P. *J. Mater. Chem.* **2000**, *10*, 127.

(17) Wallace, W. E.; Van Zanten, J. H.; Wu, W.-L. *Phys. Rev. E* **1995**, *52*, R3329.

(18) Wu, W.-L.; Van Zanten, J. H.; Orts, W. J. *Macromolecules* **1995**, *28*, 771.

(19) Van Zanten, J. H.; Wallace, W. E.; Wu, W.-L. *Phys. Rev. E* **1996**, *53*, R2053.

(20) Cecchetto, E.; De Souza, N. R.; Jérôme, B. *J. Phys. IV* **2000**, *10*, Pr7-247.

10.1021/la010811w CCC: $20.00
Published on Web 00/00/0000 PAGE EST: 5.2

Table 1. Characteristics of the PMMA Used in This Study[a]

PMMA	tacticity (%)* i/h/s	Mn (10^{-3} g/mol)	I	Tg (°C)	[η] L/mg
i-PMMA	97:03:0	37	1.21	60.6	35.7
a-PMMA	7:39:54	28.5	1.09	104	
s-PMMA	0:20:80	33	1.05	130.8	21

[a] i, h, and s represent the content of isotactic, heterotactic, and syndiotactic triads, respectively.

shown by twin neutron reflectivity that the mass density of very thin polystyrene films does not depend on the film thickness and that it is the same as the bulk value.[21] Another study showed however that density fluctuations normal to the surface might be detected by X-ray reflectivity; these fluctuations were related to the radius of gyration of the polymer.[22] Other techniques, such as positron annihilation lifetime spectroscopy[23] and more recently Brillouin light scattering[24] have suggested the existence of a surface region of different electronic density. This transition layer is assumed to play an important role in thin polymer film glass transition.

This paper gives more evidence for the existence of subtle density gradients along the normal of the surface in thin films of stereoregular PMMA. The X-ray reflectivity results exhibit a density anomaly close to the surface, a complicated transition region at the substrate/film interface, and finally a slowly undulating density depth profile.

Experimental Section

Film Preparation. The different PMMAs were synthesized by anionic polymerization to ensure well-defined tacticity, polydispersity, and molecular weight. The characteristics of the PMMA of well-defined tacticity are given in Table 1. The substrates were treated by H_2O plasma for 3 min prior to polymer deposition. The polymers were spin-cast from chloroform solutions on (111) silicon surfaces at 2000 rpm. The concentrations of PMMA solutions used were 3, 6, and 10 g/L to reach thicknesses of 25, 35, and 70 nm. The spin-coated samples were studied after annealing at Tg + 40 °C for 3 h and cooled at a constant rate. We cannot be absolutely sure that after this thermal treatment the chains within the thin films are totally relaxed. Terminal relaxation time τ_r, often called reptation relaxation time, is calculated from[25]

$$\tau_r = \frac{N^3}{N_e}\tau_0$$

where τ_0 is the average microscopic relaxation time evaluated in the order of 10^{-9} to 10^{-11} s at 160 °C, N is the degree of polymerization, namely, 350 for our PMMA, and N_e is the degree of polymerization between entanglements. N_e is 75 and 105 for s- and i-PMMA, respectively.[26] Consequently, τ_r is estimated to be inferior to 3×10^{-4} s, which is far below the 3 h annealing time applied to our samples. However, this calculated reptation time does not take into account the possible huge lowering of the relaxation time potentially induced by the pinning of PMMA segments at the SiO_x surface. Consequently, the question of whether the chains within the layer are totally relaxed or not is still unanswered.

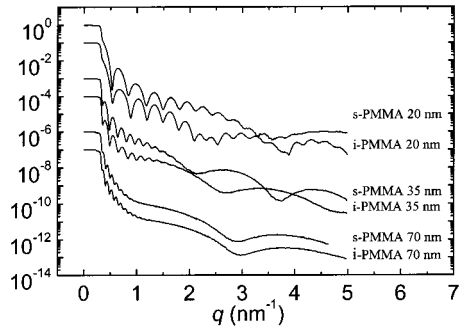

Figure 1. X-ray reflectivity curves of six different PMMA films versus momentum transfer q. From the top to the bottom, s-PMMA 20 nm, i-PMMA 20 nm, s-PMMA 35 nm, i-PMMA 35 nm, s-PMMA 70 nm, and i-PMMA 70 nm. The curves have been shifted vertically for the sake of clarity.

X-ray Reflectometry. X-ray reflectivity measurements were carried out using a Bruker-AXS D5000 diffractometer equipped with a special reflectivity stage and a graphite monochromator set for Cu $L_{3,2}$ radiation in the reflected beam. The reflectivity stage is effectively a beam-knife that cuts the beam in the center of the goniometer and thus reduces the reflective area. This area depends on the incident angle of the X-ray beam and the size of the central slit between the lower side of the beam-knife and the sample surface. With this setup, a very good resolution can be attained: film thicknesses up to 450 nm have been measured.[27] The central slit size was typically 15 microns. Step sizes and step times were variable and chosen according to the intensity measured during fast prescans in small angular intervals. Data collections were performed up to a momentum transfer $q = 4\pi \sin\theta/\lambda = 5.0$ nm^{-1}.

The physical quantity that is determined by X-ray reflectivity is the electronic density $\rho_e(z)$ normal to the sample surface. The mass density $\rho_m(z)$ can be calculated from this quantity at the condition that the composition is known:

$$\rho_m(z) = \frac{\rho_e(z)\sum_j c_j A_j}{N_a \sum_j c_j Z_j}$$

where A_j, Z_j, and c_j are the atomic mass, the atomic number, and the number fraction, respectively, of element j in the chemical formula of the polymer and N_a is Avogadro's number. For PMMA, ρ_e (in e Å^{-3}) has to be multiplied by a factor of 3.07512 to obtain ρ_m (in g cm^{-3}).

Data Fitting Procedure. The reflectivity curves in Figure 1 reveal at first sight the signature of two different periods corresponding to two distinct layers to be present. The short-range period that is mainly visible for $q < 3.0$ nm^{-1} might correspond to the total thickness of the whole polymer layer, whereas the long-range period that is mainly visible for $q > 3.0$ nm^{-1} is due to a thin native silica layer at the silicon surface with mass density $\rho_m \approx 1.9$ g cm^{-3}.[28] This has been confirmed by running experiments on a bare plasma-treated silicon wafer where only the long-range period is observed. Analysis of the reflectivity curves was however not successful using either Parrat's recursive equations[29] or traditional least-squares methods supposing only a two-layer model. Therefore, several alternative inversion schemes were tried that claim to be more or less model-independent.[22,30−34] The best results were obtained

(21) Wallace, W. E.; Beck Tan, N. C.; Wu, W.-L.; Satija, S. K. *J. Chem. Phys.* **1998**, *108*, 3798.
(22) Sanyal, M. K.; Basu, J. K.; Datta, A.; Banerjee, S. *Europhys. Lett.* **1996**, *36*, 235.
(23) DiMaggio, G. B.; Frieze, W. E.; Gidley, D.; Zhu, W. M.; Hristov, H. A.; Yee, A. F. *Phys. Rev. Lett.* **1997**, *78*, 1524.
(24) Mattsson, J.; Forrest, J. A.; Börjesson, L. *Phys. Rev. E* **2000**, *62*, 5187.
(25) de Gennes, P. G. *Scaling Concepts in Polymer Physics*; Cornell University Press: Ithaca, NY, 1979.
(26) Jasse, A. K.; Oultache, H.; Mounach, J. L.; Halary, L. M. *J. Polym. Sci., Part B: Polym. Phys.* **1996**, *34*, 2007.
(27) Van der Lee, A.; Roualdes, S.; Berjoan, R.; Durand, J. *Appl. Surf. Sci.* **2001** *173*, 115.
(28) Tolan, M.; Seeck, O. H.; Wang, J.; Sinha, S. K.; Rafailovich, M. H.; Sokolov, J. *Physica B* **2000**, *283*, 22.
(29) Parrat, L. G. *Phys. Rev.* **1954**, *95*, 359.
(30) Pedersen, J. S.; Hamley, I. W. *J. Appl. Crystallogr.* **1994**, *27*, 36.
(31) Sanyal, M. K.; Hazra, S.; Basu, J. K.; Datta, A. *Phys. Rev. B* **1998**, *58*, 425.
(32) Berk, N. F.; Majkrzak, C. F. *Phys. Rev. B* **1995**, *51*, 11296.
(33) Li, M.; Möller, O.; Landwehr, G. *J. Appl. Phys.* **1996**, *80*, 2788.

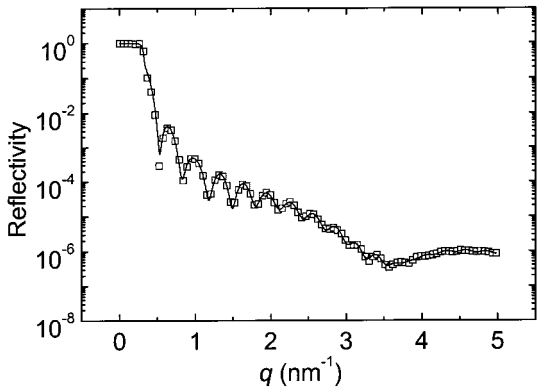

Figure 2. Superposition of experimental and simulated X-ray reflectivity curve of a 25 nm thin film of s-PMMA. The squares represent the experimental data, and the full line represents the fitted curve.

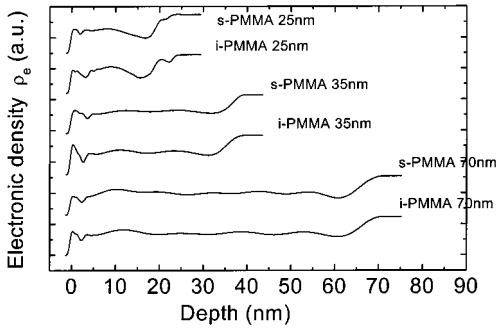

Figure 3. Simulated electronic density versus depth for six different PMMA films. From the top to the bottom, s-PMMA 20 nm, i-PMMA 20 nm, s-PMMA 35 nm, i-PMMA 35 nm, s-PMMA 70 nm, and i-PMMA 70 nm. The curves have been shifted vertically for the sake of clarity. The three distinct regions under discussion are the film−air interface (left of the first dashed line), the density fluctuations in the film (in between the two dashed lines), and the film−silicon interface (right of the second dashed line), from the left to the right.

using a slightly adapted form of Sanyal's distorted wave Born approximation based fitting method.[22] The accuracy of the method is pointed out in Figure 2 where the fitted curve is superimposed on the experimental reflectivity curve for a 75 nm thin layer of s-PMMA.

The slice thickness Δz used in the calculations was chosen according to the real-space resolution of the experiment, that is, $\Delta z = \pi/q_{max}$. Sanyal's other method, the one based on the Born approximation,[31] yielded slightly different density profiles but with the same characteristics. The final profile depends on the actual starting point, that is, the mean electronic density value of the film. Two slightly different profiles could give nearly identical fits, showing that the solution is never completely unambiguous.[34] The off-specular scattering was measured as well to evaluate the roughness due to in-plane height−height correlation. This scattering was found to be very low, so it can be concluded that the density profiles presented in Figure 3 are solely due to diffuseness, that is, vertical electron density gradients. This results in relatively complex density profiles for which the physical meaning has to be interpreted.

Results and Discussion

Three different features can be distinguished in Figure 3: (i) the rather short-scale density fluctuations at the substrate−film interface, (ii) the likewise short-scale fluctuations at the air−film interface, and (iii) the slow undulations in the bulk of the film. These effects will be discussed hereafter in this order.

Density Profile at the Film−Silicon Interface. As observed in Figure 3, the stabilization of the density at the film/substrate interface occurs at roughly 1.9 g cm^{-3} which is the density of the native oxide silica layer. A gradual increase in the mass density, as compared to the bulk, is observed in the vicinity of the silicon surface, namely, between 5 and 10 nm from the wall whatever the film thickness and PMMA tacticity. This region is located at the right of the second dashed vertical line for each thickness of the film. The same phenomenon is also observed for a conventional atactic PMMA film. This density increase is consistent with observations made by other workers on PMMA by neutron reflectometry,[18] X-ray reflectivity,[15] or fluorescence.[35] Molecular simulation[36−38] has also provided similar results even for noninteracting polymer/surface systems. From these computer simulations and calculations, a thin interfacial layer with altered density is highlighted and the density drops to the bulk value after a few nanometers. The authors argue that the coils' shape can be distorted near a surface such that their dimension perpendicular to the surface must be decreased and their dimension in the plane of the surface is increased. This flattening of the chains is accompanied by an increase in the segment density near a wall, which results from interplay between factors acting in the opposite direction. It is well established that the loss of configurational entropy due to the presence of an impenetrable wall is a repulsive factor for a polymer chain, which tends to favor a depletion of the region near the surface. In contrast, the monomer/surface adhesion force is an attractive factor that depends on the nature of the interfacial interactions. Other parameters, put forward in the case of a noninteracting wall, are the packing constraints that are exerted, at meltlike densities, by the chains in the matrix, which press the chains present near the interface against the wall.[38] The polymer chains will, therefore, align parallel to the surface, reduce their orientational entropy, and increase the monomer density near the film/substrate interface. Chain stiffness disparity also plays a significant role on the so-called entropy-driven surface segregation of stiffer chain segments[39] which can, in turn, enhance the monomer density near a wall. Contradictory experimental results are available in the literature on the possible alteration of chain characteristics at an interface. Whereas the modification of the chain conformation (local conformation, persistence length) in a thin film is generally accepted,[1,40,41] the distortion of the shape of the coil is still controversial.[42,43]

PMMA is known to strongly interact with the SiO_x surface through acid−base interactions.[12] These attractive interactions represent a significant driving force for enhancing the monomer density in the interfacial region. Moreover, PMMA is constituted of segments of different stereoregularity which influence the chain stiffness by modifying the local conformation of the chain.[44] Even

(34) Luokkala, B. B.; Garoff, S.; Suter, R. M. *Phys. Rev. E* **2000**, *62*, 2405.
(35) Lipatov, S. Y.; Moisya, E. G.; Semenovich, G. M. *Polymer* **1975**, *16*, 582.
(36) Dickman, R.; Hall, C. K. *J. Chem. Phys.* **1988**, *89* (5), 3168.
(37) Mansfield, K. F.; Theodorou, D. N. *Macromolecules* **1989**, *22*, 3143.
(38) Binder, K.; Baschnagel, J.; Bohmer, S.; Paul, W. *Philos. Mag. B* **1998**, *77* (2), 591.
(39) Yethiraj, A.; Kumar, S.; Hariharan, A.; Schweizer, K. S. *J. Chem. Phys.* **1994**, *100* (6), 4691.
(40) Grohens, Y.; Brogly, M.; Labbe, C.; Schultz, J. *Polymer* **1997**, *38* (24), 5913.
(41) Brûlet, A.; Boué, F.; Menelle, A.; Cotton, J. P. *Macromolecules* **2000**, *33*, 997.
(42) Shuto, K.; Oishi, Y.; Kajiyama, T. *Polymer* **1995**, *26* (3), 549.
(43) Jones, R. L.; Kumar, S. K.; Ho, D. L.; Briber, R. M.; Russel, T. *Nature* **1999**, *400*, 146.
(44) Vacatello, M.; Flory, P. J. *Macromolecules* **1986**, *19*, 405.

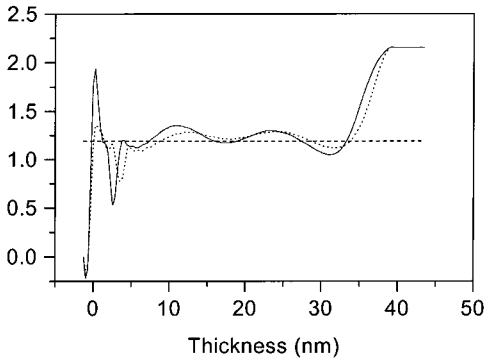

Figure 4. Mass density versus depth for a 35 nm i-PMMA film (full line) and s-PMMA film (dotted line). The dashed straight line represents the bulk density of conventional a-PMMA given as a reference.

atactic PMMA exhibits local disparities in flexibility since at least 50% of the chains are made of syndiotactic triads. For instance, we already mentioned in previous work[45] that stereospecific adsorption of isotactic sequences can occur at the chloroform/silica interface. Strong interactions and stereospecific adsorption are likely to enhance local packing of PMMA chain segments of similar tacticity near an attractive surface such as SiO_x-covered silicon as observed in Figure 3.

Density Profile at the Film−Air Interface. From Figure 3, an increase in density is also observed, at the left of the first dashed vertical line, in the vicinity of the film/air interface, followed by a decay in the electron density, ρ_e, at both sides of this density peak. At the left side, the sharp decrease of the density corresponds to the transition from the polymer material to the air. The existence of a surface roughness of the film makes it difficult to determine the exact location of the film/air interface according to the depth axis. At the right side of the peak, a depletion zone results from the layering effect which will be discussed later. Since no interactions are expected at this interface, the only driving force for the enhanced packing might be the surface segregation of stiffer chain segments as claimed by Yethiraj et al.[39] These results obtained from computer simulations are consistent with ToF-SIMS experiments carried out by Bertrand et al.[46] on films of PMMA who showed, from the extracted fragments, significant conformational differences at the free surface according to the polymer tacticity. Tretinnikov[47] also evidenced water contact angles that were highly stereoregular sensitive on the free surface of PMMA film according to the surface on which it was previously cast. Conformations as well as packing of chain segments at the free interface are, therefore, assumed to be entropy-driven. However, the role of surface segregation of impurities or low molecular weight compounds in the complexity of the density profile at the free surface cannot be totally ruled out; therefore, this point deserves further investigation.

Density Periodic Fluctuation in the Thin Film. In subsequent layers, close to the regions of enhanced density at both interfaces, zones of reduced density are observed between the two dashed vertical lines. In our experiments, this is clearly observed for the 25 nm layer in Figure 3 but also shown in Figure 4 from the superposition of the mass density profiles of i- and s-PMMA thin films of 35 nm. The mass density oscillates with depth around the bulk density of a conventional a-PMMA, namely, 1.19 g/cm^{-3}, represented in Figure 4 as a dashed straight line.

The interpretation of the physical signification of these depletion layers is not straightforward. Sanyal et al.[22] were the first to observe this periodic layering of high and low electron density. Other authors mentioned that layering of liquid atoms, such as Hg or Ga,[48,49] could occur as a function of depth due to short-range anisotropic ordering close to a surface. Thermally excited capillary waves at an interface are suggested to largely contribute to this layering effect. It is also striking to observe that the periodicity of the density fluctuation is slightly different for the two PMMA stereoisomers. Actually, in thin films of 70 nm, the wavelength of the density oscillation is on average 10 and 15 nm for s- and i-PMMA, respectively. These values are close to the radius of gyration of both PMMA stereoisomers coils in their respective θ conditions. Sanyal et al.[22] suggested that part of the chain could be grafted to the substrate and that the rest is in a coiled configuration such as in a mushroom configuration. However, they did not give further arguments for explaining the physical meaning of their interesting results. Beside, several groups[3,8,50,51] have suggested that modification in the degree of interpenetration of the polymer coils near an interface could occur, and we feel that this could contribute to the observed layering effect.

The arguments put forward hereafter are valid for the observed depletion layer at both interfaces as well as for the oscillating density fluctuation observed for layers thicker than 35 nm. Actually, fluorescence experiments carried out by Chang and Morawetz[54] and more recently by Chen et al.[55] on freeze-dried solutions suggest that chain interpenetration is negligible for dilute solutions, $c < 1/[\eta]$, and then increases but seems to encounter a strong resistance for further interpenetration at a concentration above c^* which is the critical concentration separating the dilute from the semidilute regimes. This would generate long-range density inhomogeneities in semidilute solutions. The key idea drawn from the results obtained by Morawetz is that the material retains a certain memory of the chain interpenetration that had existed in the original solution due to the rapid freezing of chain conformations. The overlapping concentration is roughly 10 g/L for the PMMA in chloroform, which corresponds to the highest concentration used in our study. Graessley[56] has shown that the molecular weight between entanglements (M_e) is inversely proportional to the polymer weight fraction in solution:

$$M_e^{sol} \sim M_e^{melt}/\phi$$

where M_e^{sol} is the molecular weight between entangle-

(45) Carriere, P.; Grohens, Y.; Spevacek, J.; Schultz, J. *Langmuir* **2000**, *16* (11), 5051.
(46) Vanden Eynde, X.; Weng, L. T.; Bertrand, P. *Surf. Interface Anal.* **1997**, *25*, 41.
(47) Tretinnikov, O. N. *J. Adhes. Sci. Technol.* **1999**, *13* (10), 1085.
(48) Regan, M. J.; Kawamoto, E. H.; Lee, S.; Pershan, P. S.; Maskil, N.; Deutsch, M.; Magnussen, O. M.; Ocko, B. M.; Berman, L. E. *Phys. Rev. Lett.* **1995**, *75* (13), 2498.
(49) Magnussen, O.; Ocko, B. M.; Regan, M. J.; Penamen, K.; Pershan, P. S.; Deutsch, M. *Phys. Rev. Lett.* **1995**, *74* (22), 4444.
(50) Sauer, B. B.; Walsh, D. J. *Macromolecules* **1994**, *27*, 432.
(51) Overney, R. M.; Buenviaje, C.; Luginbuhl, R.; Dinelli, F. *J. Therm. Anal. Calorim.* **2000**, *59*, 205.
(52) Buenviaje, C.; Shouren, G.; Rafailovich, M.; Sokolov, J.; Drake, J. M.; Overney, R. M. *Langmuir* **1999**, *15* (19), 6449.
(53) Zeng, X.; Rafailovich, M. H.; Sokolov, J.; Strzhemechny, Y.; Schwarz, S. A.; Sauer, B. B.; Rubinstein, M. *Phys. Rev. Lett.* **1997**, *79*, 241.
(54) Chang, L. P.; Morawetz, H. *Macromolecules* **1987**, *20*, 428.
(55) Chen, J.; Xue, G.; Li, Y.; Wang, L.; Tian, G. *Macromolecules* **2001**, *34*, 1297.
(56) Graessley, W. W. *Adv. Polym. Sci.* **1974**, *16*, 58.

ments in solution, M_e^{melt} is the molecular weight between entanglements in the melt, and ϕ is the polymer weight fraction. For the 10 g/L solution, the entanglement density would be reduced by 2 orders of magnitude as compared to the bulk. Sauer et al.[50] suggest that the chains collapse in a less entangled state and are frozen in this state because of the rapid solvent removal. The enthalpy of vaporization per mole of the organic solvent used for the spin coating, namely, roughly 30 kJ/mol, combined with the fast rotation of the sample allows very fast evaporation of the residual solvent that has not been removed by the centrifugal forces. Therefore, the temperature of the film can be expected to drop by at least 30 °C. Some kind of freeze-drying during the formation of the thin film could, therefore, account for a reduction in the chain interpenetration as compared to bulk samples. In thin films, several workers[51−53,57] provided the interpretation of a reduced degree of entanglement. Overney et al.[51] from nanomechanical measurements suggested that a low-density region at the interface could result from a gel-like structure less entangled than a melt. These authors also claimed[52] that a disentangled 20 nm porelike sublayer exists at the silicon interface followed by a less entangled boundary layer. According to these workers, this effect is ascribed to the spin-coating process and propagates 7−10 Rg apart from the substrate. From diffusion experiments[53] of hPS and dPS followed by dynamic SIMS experiments, the degree of entanglement was also considered as a possible mechanism to propagate the influence of the interface through a thin film. In our belief, the correlation between the degree of entanglement and the density fluctuations remains unclear and would necessitate much more experimental and theoretical investigations from the thin film scientific community. An experimental approach to try to validate this assumption will be to make thin films from the freeze-dying process and study their density profiles and glass transition temperature.

The foregoing interpretation of the layering phenomena does however not explain why the annealing time at $T \gg$ Tg is not sufficient to attain an equilibrium entanglement density. Indeed, the rate of reentanglement is related to the reptation time, τ_r, which was calculated to be in the order of 3×10^{-4} s at 160 °C. Therefore, other tentative explanations might be found. Actually, the mutual interpenetration of polymer chains could be limited due to the entropy loss due to confinement in thin layers or at polymer interfaces. The loss of entropy of the adsorbed layer could experience a repulsive force on the overcoming chains from differences in the entropy with the surface attached chains. A fascinating experience illustrating this effect was carried out by Reiter[57] between chemically identical polymers showing that entropy-driven dewetting of PS cast on a PS brush occurs even below the bulk polymer Tg. Indeed, strongly stretched PS chains of the brush, chemically attached to the surface, have a lower number of possible conformations (lower entropy) than the one cast above yielding a higher mobility of the top polymer layer. In our study, 25 nm is the lower thickness necessary to achieve stability of the film even after several annealing treatments at $T >$ Tg. For film thickness below 20 nm, holes appear in the layer during heating which are ascribed to dewetting phenomena. From AFM investigations in the friction mode (LFM, lateral force microscopy), the calculated friction coefficient inside the holes is significantly different than that of the bare silicon surface, namely, 0.40 and 0.29, respectively.[58] Moreover, the friction coefficient inside the holes is identical to that of the PMMA surface. From these experiments, it is concluded that adsorbed polymer is still present in the bottom of the holes. This is consistent with the assumption of a disentanglement of polymer chains in thin layer presumably resulting from a so-called autophobic effect[59] leading to an entropically driven incompatibility between the adsorbed and nonadsorbed chains.

De Gennes[25] proposed that excluded volume interactions that do not exist in the bulk polymer could be generated in supported thin films due to the presence of a solid surface. Indeed, the distortion of the coil spherical shape (cigarlike) near a surface induces expulsion of a given amount of chain segments of interpenetrating chains in the direction perpendicular to the surface. The removal of the interpenetrating segments which in the bulk experiences a screening of the monomer−monomer interactions for segments belonging to the same chains yield excluded volume repulsive interactions such as in athermal solvents. The limitation of coil interpenetration by long-range repulsive interactions could result in depletion zones alternating with higher density regions. The same situation is assumed in a semidiluted solution in a good solvent where above the overlap concentration C^*, the interpenetration of polymer coils is limited by the favorable polymer/solvent interactions.

The average density $\rho_m(h)$ of the thin films can be deduced from the calculated density profiles according to the polymer tacticity. This average density is calculated between the zero depth corresponding to the film/air interface and the depth at which the density of the silicon oxide is reached. This density of 1.9 g cm^{-3} is taken as representative of the film/silicon interface. $\rho_m(h)$ is 1.25 and 1.24 for 70 nm films, 1.28 and 1.25 for 35 nm films, and 1.32 and 1.28 for 20 nm films of i- and s-PMMA, respectively. These calculated densities are higher than the bulk density of amorphous PMMA which is 1.19 g cm^{-3} whatever the film thickness. This conclusion is consistent with that drawn by Wu et al. on PMMA thin films on silicon[18] but in disagreement with results obtained by Wallace et al. for PS on silicon[21] who did not find any density variation in thin films. We are aware that our average density could be somewhat overestimated since the transition between the density of the PMMA film and the density of the silicon oxide at 1.9 g cm^{-3} is rather sharp. However, our results can be discussed in a comparative way. Thus, the PMMA density increases when the film thickness decreases and the density of i-PMMA in thin films is always higher than that of s-PMMA. However, the correlation of these results with the glass transition temperature, Tg(h), of thin layers of stereoregular PMMA is not straightforward. Our previous results[12] showed that i-PMMA exhibits an increase of the Tg(h) for thicknesses below 50 nm whereas a Tg(h) depression is observed for s-PMMA as compared to the bulk value. Moreover, Tg(h) tends to the same unique value of 100 °C for a thickness of 25 nm. We assume that modification in Tg(h) in thin layers is not directly correlated to the average density of the film but rather to the density fluctuations. Indeed, these fluctuations are revealing changes in chain interpenetration and, therefore, chain conformation which are known to influence structural relaxation.[54] Therefore, the rate of structural relaxation is perhaps a key parameter in the measured Tg in thin films as will be discussed in a forthcoming paper.

To summarize our work, many physical arguments can be put forward to explain the density oscillations observed

(57) Reiter, G.; Auroy, P.; Auvray, L. *Macromolecules* **1996**, *29*, 2150.
(58) Grohens, Y.; Hamon, L.; Castelein, G.; Holl, Y. *Macromolecules*, submitted.
(59) Hare, E. F.; Zismann, W. A. *J. Phys. Chem.* **1955**, *59*, 335.

from our X-ray reflectometry experiments. Further experiences are required to get insights about the real driving force of these density gradients at interfaces and density fluctuations. The nature of the solvent used for spin coating, the nature of the polymer, and the chemical treatment of the surface are experimental factors which will be examined. Moreover, an ab initio methodology of X-ray data analysis, independent of any model density profile, will also be used to validate these density profiles in the near future.

Conclusion

X-ray reflectivity curves from very thin PMMA films that could not be properly analyzed by traditional fitting methods have been treated by an alternative method based on the distorted wave Born approximation. The resulting density profiles clearly evidenced subtle density fluctuations normal to the surface that have already been suggested by other authors. The increased density near the silicon surface and at the free surface is ascribed to better chain packing due to interfacial interactions and selective adsorption of stereoregular sequences, respectively. The density fluctuations are ascribed to a layering of polymer coils partially disentangled in polymer films. The relation between the density fluctuation and the existence of a specific glass transition temperature of the polymer in a thin layer is not straightforward and will deserve further investigations.

LA010811W